Fuel 188 (2017) 367–373

Contents lists available at ScienceDirect

Fuel

journal homepage: www.elsevier.com/locate/fuel

Full Length Article

Permittivity of diesel fossil fuel and blends with biodiesel in the full range from 0% to 100%: Application to biodiesel content estimation

J. Corach [a], P.A. Sorichetti [b], S.D. Romano [a,*]

[a] Universidad de Buenos Aires, CONICET, Instituto de Tecnología del Hidrógeno y Energías Sostenibles (ITHES), Facultad de Ingeniería, Departamento de Ingeniería Mecánica, Grupo de Energías Renovables (GER), Buenos Aires, Argentina
[b] Universidad de Buenos Aires, Facultad de Ingeniería, Departamento de Física, Laboratorio de Sistemas Líquidos (LSL), Buenos Aires, Argentina

HIGHLIGHTS

- The permittivity of diesel fuel and blends with biodiesel was determined at 100 kHz.
- The measurement uncertainty was below 1%.
- Linear dependences with temperature and composition were found.
- Composition is estimated from permittivity and temperature measurements.
- The RMS uncertainty of biodiesel content estimation is below 2.5%.

ARTICLE INFO

Article history:
Received 2 July 2016
Received in revised form 26 September 2016
Accepted 2 October 2016

Keywords:
Permittivity
Dielectric spectroscopy
Blends
FAME
Biodiesel
Diesel fuel

ABSTRACT

The relative permittivity of diesel fossil fuel and blends with biodiesel from soybean, in the full range from pure diesel to 100% biodiesel, was determined at temperatures between 298.0 K and 333.0 K (controlled within ±0.1 K), using an airtight cell. Measurements were made in the frequency range from 1 kHz to 100 kHz; this frequency range is suitable for the use of low-cost, portable equipment and also for the development of automotive sensors. The relative uncertainty of the measurements was below 1%.

Experimental values of permittivity were satisfactorily fitted to a simple model as a function of temperature and composition. The RMS uncertainty of the fitting was 1.2%. The model parameters were determined from experimental results and verified by multiple regression analysis, with very good agreement.

In addition, a model was proposed to estimate the composition of diesel/biodiesel blends from permittivity and temperature measurements. The parameters of the model were obtained by a multiple regression analysis; the RMS uncertainty of the composition estimation was below 2.5%.

The results presented in this work describe accurately the dependence of the permittivity of diesel fuel with temperature and also validate and extend previously reported models for biodiesel-rich blends with diesel fossil fuel, allowing the estimation in the full composition range with good accuracy.

1. Introduction

Diesel fossil fuel (DF) has been widely used for many years in automotive and stationary applications. Since the last decades, the use of biodiesel (BD) as a renewable alternative [1–3], pure or in blends with DF, has increased rapidly all around the world due to environmental concerns, including the reduction of carbon dioxide emissions. In consequence, there is renewed interest in the development of low-cost, fast and accurate liquid fuel characterization techniques that can be adapted to small-scale production plants, distribution points and field measurements, particularly in emerging markets. Dielectric [2,4] and ultrasonic [5,6] techniques are promising alternatives in that direction. In particular, dielectric spectroscopy has been successfully used for the production and characterization of BD [2] and also to characterize feedstocks from different origins [7,8]. They have also been used to detect alcohol in the light phase after transesterification [9], during the purification process and in the final product

* Corresponding author at: ITHES (UBA – CONICET) – GER (Grupo de Energías Renovables), Facultad de Ingeniería, Universidad de Buenos Aires (UBA), Av. Paseo Colón 850, Ciudad Autónoma de Buenos Aires 1063, Argentina.
E-mail addresses: sromano@fi.uba.ar, silviadromano@gmail.com (S.D. Romano).

http://dx.doi.org/10.1016/j.fuel.2016.10.019
0016-2361/

[10,11], for the characterization of fatty acid methyl esters (FAME) [12,13] and to distinguish between vegetable oil and the biodiesel produced from it [6].

The determination of the composition of DF/BD blends is very important for legal, commercial and technical reasons. Legal and commercial issues include the verification of the actual BD content in DF/BD blends; for instance, legislation in many countries establishes that diesel fossil fuel (DF) must be blended with a certain amount of BD (usually up to 20%). Moreover, the blend composition impacts engine performance and emissions [14]. The composition of a DF/BD blend is usually indicated as "*Bx*", where "x" represents the percentage of BD (V/V). For example, B0 means pure DF and B100 means pure BD. The determination of *Bx* by standard methods [15] is usually expensive, time-consuming, requires trained personnel and it is not easily adaptable to real-time measurement systems. Also, they cannot be used for in situ measurements (for instance during fuel storage and transportation). On the other side, dielectric measurements are a low-cost and fast alternative, which does not require highly trained personnel.

It must be remarked that the development of dielectric characterization techniques for DF/BD blends requires the accurate measurement and modeling of the temperature dependence of the permittivity in the full composition range. Interestingly, although some works report DF permittivity values [4,11], the authors have not found in the literature explicit models of the dependence of DF permittivity on temperature.

An early work by Tat and Van Gerpen, [16], explored the use in biodiesel blends (B0 to B100) of a commercial dielectric sensor originally designed for methanol-gasoline blends; the device operated at room temperature (296 K). The uncertainty of the composition determination was ±10%; the permittivity values of the samples were not reported. Munack at al. [4] described a sensor specifically designed for the determination of the composition of DF/BD blends (B0 to B100) in automotive applications. Graphs of permittivity values were plotted for temperatures of 278 K, 303 K and 323 K, at a frequency of 1 kHz. The sensor was successfully tested in a passenger car covering more than 50,000 km of on-the road use. The precision of blend detection was ±10%. In [17], De Souza et al. reported permittivity and conductivity measurements of DF/BD blends (B0 to B10) at frequencies between 0.1 Hz and 100 kHz at room temperature. In a previous work [18] the authors studied the dielectric properties of biodiesel-rich blends with diesel fuel (B50 to B100) at temperatures between 303.0 K and 343.0 K at frequencies between 20 Hz and 2 MHz. From these results, a model for the estimation of the composition of BD rich blends from permittivity and temperature measurements was presented. The RMS uncertainty of the estimation was below 1.5% in the full temperature and composition ranges studied.

In this work, the permittivity of pure DF, BD and their blends was measured in an airtight cell, for samples in the full composition range from 0% to 100% (V/V) of BD, at temperatures from 298.0 K to 333.0 K, between 1 kHz and 100 kHz. The range of measurement frequencies in this work makes possible the use of low-cost, portable equipment and it is also useful for the development of sensors for automotive applications, using state-of-the-art electronics. From the experimental results, a model was proposed to estimate the permittivity as a function of composition and temperature with an RMS uncertainty below 1.2%. Furthermore, a simple model is proposed for the estimation of blends composition from permittivity and temperature measurements. The RMS uncertainty of the composition estimation is below 2.5% in the full range of temperatures and compositions.

The results and models presented in this work validate and extend those presented in [18] to the full range of compositions. They are relevant for the design and implementation of accurate, economical and compact measurement systems.

2. Samples and methods

2.1. Samples

All the samples were prepared with commercial BD from soybean oil provided by a local producer, certified to met standard EN 14214 [19]. Certified pure DF samples were also provided by a local producer and also complied with international standards [20]. Since the BD and DF used for sample preparation were certified by their producers, no pre-processing procedures were carried out.

2.2. Measurement system

The relative permittivity of the samples was determined from isothermal dielectric measurements between 1 kHz and 100 kHz with a LCR meter (Tonghui TH2822C). The measurement cell is airtight to prevent systematic errors due to evaporation of the sample. To minimize polarization effects, the electrodes are made of platinized platinum. During the measurement, the cell is immersed in a thermostatic bath (Lauda), allowing a very precise temperature control (within ±0.1 K) and avoiding systematic error due to thermal gradients. Fig. 1 shows the main characteristics of the experimental setup, including the circuit configuration and the cell diagram. The system was calibrated with an uncertainty below 1% using cyclohexane as a reference liquid. All the uncertainties in this work are given as one standard deviation. The measurement uncertainty of real part of permittivity, $\Delta\varepsilon_r'$, was below 1% in all cases. In this work all the uncertainties were obtained from the statistical analysis of experimental data. Relative permittivity experimental values at each frequency were obtained as the average of 3 sets of 30 repetitions each; it must be remarked that the difference in the average values of each set was well below 1%. Besides, since no statistically significant differences in the permittivity values were observed between measurements at 1 kHz, 10 kHz and 100 kHz, the results reported in this work correspond to 100 kHz. It is important to note that measurements at this frequency minimize the influence of electrodes polarization that could occur in deficiently purified FAME samples.

In all the cases presented in Section 4, the uncertainty of the linear fittings parameters (from Eqs. (1)–(3)) was from the least-squares fitting to experimental data. The overall uncertainty of the models from Eqs. (4)–(6) was estimated as the RMS error between the experimental data and the estimated values.

3. Theory

3.1. Electrical properties

The dielectric properties of the samples are described by the relative permittivity as a function of temperature and composition [2,21,22]. As it was to be expected from results in previous works [6,18], given the high purity of the samples, it was experimentally found that dielectric losses in the frequency range studied could be neglected. Also, it was found that permittivity measurements at each composition fit very satisfactorily to a linear dependence with the absolute temperature of the sample, T:

$$\varepsilon_r'(Bx_o, T) = \varepsilon_r'(Bx_o, T_o) + \frac{\delta\varepsilon_r'(Bx_o, T_o)}{\delta T}(T - T_o) \quad (1)$$

In Eq. (1), $\varepsilon_r'(Bx_o, T)$ is the relative permittivity of a sample with composition Bx_o at temperature T. The reference temperature is T_o = 318.0 K. The temperature coefficient of the relative permittivity, $\frac{\delta\varepsilon_r'(Bx_o,T_o)}{\delta T}$, is given in K^{-1} at the reference temperature, T_o, and at the reference composition, B0.

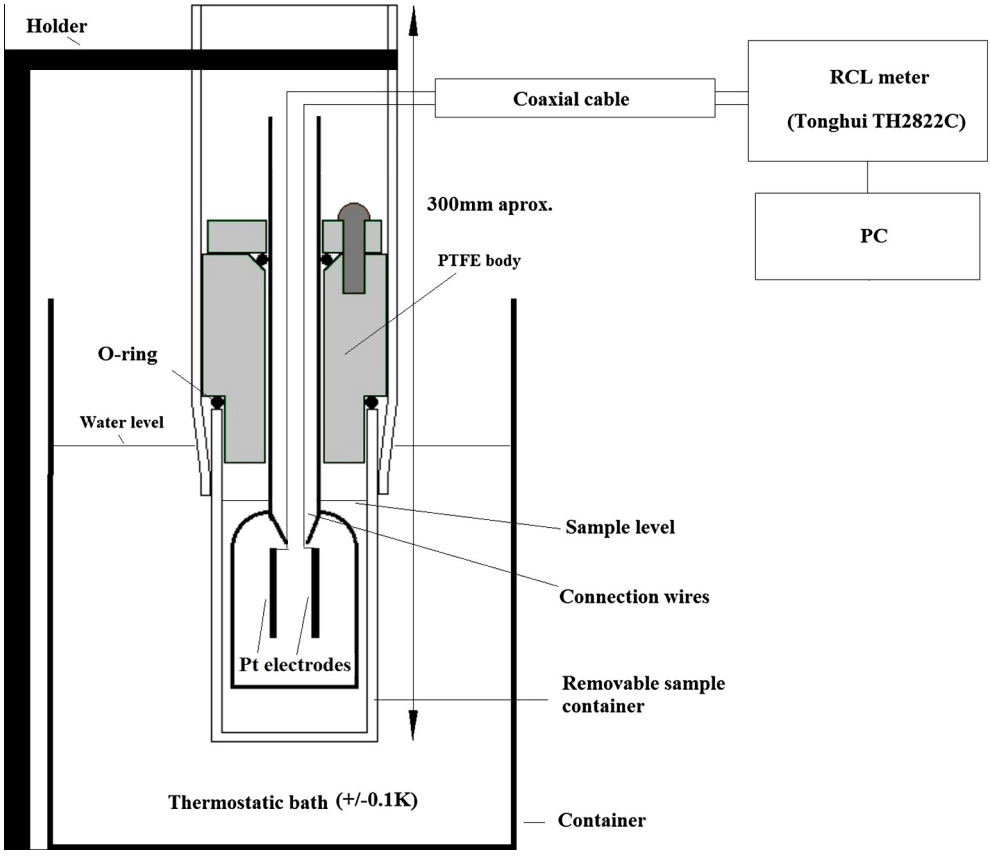

Fig. 1. Experimental setup.

Similarly, in the full range of compositions, permittivity experimental data are accurately modeled by a linear dependence on composition:

$$\varepsilon_r'(Bx, T_o) = \varepsilon_r'(B0, T_o) + \frac{\delta\varepsilon_r'}{\delta Bx} Bx \tag{2}$$

where $\varepsilon_r'(B0, T_o)$ is the permittivity value of pure DF at the reference temperature, T_o, and $\frac{\delta\varepsilon_r'(Bx_o, T_o)}{\delta T}$ is evaluated at the reference temperature T_o and at the reference composition B0.

From experimental results in the full range of temperatures and compositions, it is found that $\delta\varepsilon'_r/\delta Bx$ depends linearly on temperature:

$$\frac{\delta\varepsilon_r'(T)}{\delta Bx} = \frac{\delta\varepsilon_r'(T_o)}{\delta Bx} + \frac{\delta^2\varepsilon_r'}{\delta Bx\delta T}(T - T_o) \tag{3}$$

In this work $\delta\varepsilon'_r(T_o)/\delta Bx$ and $\delta^2\varepsilon'_r/\delta Bx\delta T$ were determined by means of a linear regression on T.

From Eqs. (1)–(3), the permittivity as a function of temperature and composition may be estimated by

$$\varepsilon_r'(Bx, T) = \varepsilon_r'(B0, T_o) + \frac{\delta\varepsilon_r'(B0, T_o)}{\delta T}(T - T_o) + \left[\frac{\delta\varepsilon_r'(T_o)}{\delta Bx} + \frac{\delta^2\varepsilon_r'}{\delta Bx\delta T}(T - T_o)\right] Bx \tag{4}$$

The model of Eq. (4) had been proposed and validated for biodiesel-rich blends ($Bx \geqslant 50\%$) in a previous work [18]. In this paper the model was validated for the full composition range (B0 to B100) by experimental results from pure DF and DF-rich blends with BD, using an improved, airtight cell, at a frequency of 100 kHz.

4. Results and discussion

4.1. Electrical properties of diesel blends with biodiesel

Fig. 2 shows a three dimensional plot of the real part of the permittivity of the DF/BD samples as a function of temperature, T, and composition, Bx. Uncertainty error bands are smaller than the markers. The values corresponding to B10 (328 K), B20 (313 K)

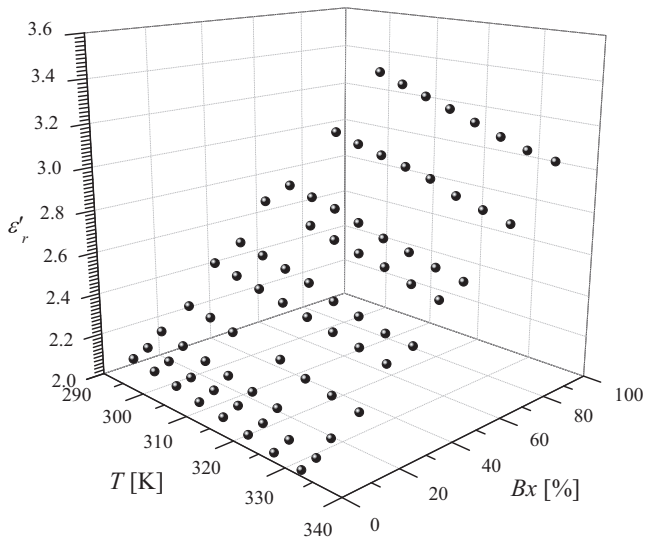

Fig. 2. Experimental values of relative permittivity, ε_r', of DF/BD blends as a function of biodiesel content, Bx, and temperature, T.

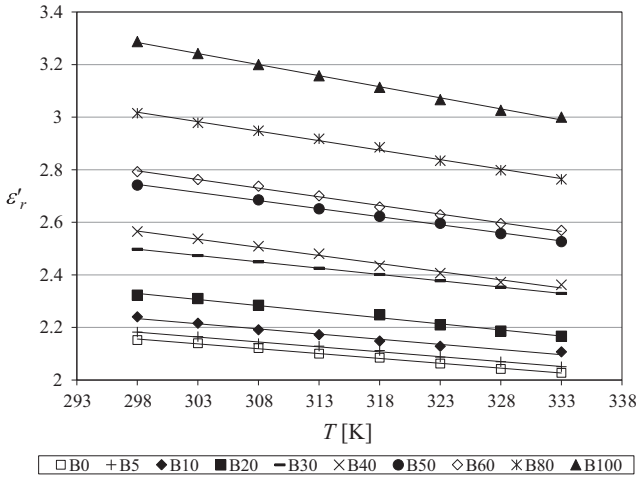

Fig. 3. Projection of the experimental values (symbols) of ε_r' onto the (ε_r', T) plane. The lines correspond to the fitting of $\varepsilon_r'(Bx, T)$ to Eq. (1).

and B50 (303 K) were discarded because of electrical noise effects during measurements.

The surface $\varepsilon_r'(Bx, T)$ may be projected onto the (ε_r', T) and (ε_r', Bx) planes in order to analyze the dependence of ε_r' on T, at each composition, Bx_o, and on Bx, at a fixed temperature T_o.

Fig. 3 shows experimental values of ε_r' as a function of temperature for all the studied samples (projection onto the (ε_r', T) plane). The symbols correspond to the different compositions. The continuous lines represent the fitting of the linear model, Eq. (1), for each sample.

As in the case of biodiesel-rich blends with DF [18], ε_r' decreases linearly with temperature for all the compositions and, at a given temperature, increases with Bx. Table 1 shows the fitting parameters of Eq. (1) for all the samples studied in this work. The values of $\varepsilon'_r(T_o)$ and $\delta\varepsilon'_r/\delta T$ are given together with their uncertainties, $\Delta\varepsilon'_r(T_o)$ and $\Delta\delta\varepsilon'_r/\delta T$. The RMS uncertainty of the fitting, $\Delta\varepsilon'_r$, and the determination coefficient, R^2, are also shown. The reference temperature is T_o = 318.0 K.

From Table 1 it is easy to see that both $\varepsilon'_r(T_o)$ and the magnitude of the slope ($\delta\varepsilon'_r/\delta T$) increase with Bx. This was to be expected since BD is a more polar substance than DF [2,11]. As in the case of pure BD [2,6,11], vegetable oils [2,8] and biodiesel-rich blends with diesel fossil [18], the permittivity of pure diesel fuel (B0) and diesel-rich blends decrease linearly with temperature. The experimental results in this work make possible to extend the validity of the model of Eq. (1), previously proposed for blends from B50 to B100 [18], to the full composition range. Diesel-rich blends (up to B20) are of particular interest for automotive applications. Fig. 4 shows in more detail the fitting of experimental values of ε'_r (symbols) to the linear model (Eq. (1)) of B0 and B20 samples.

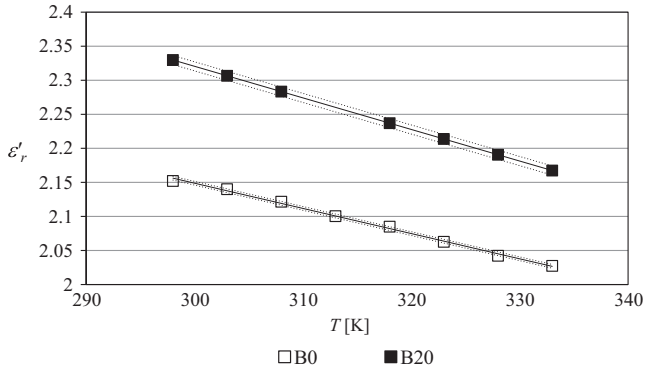

Fig. 4. Relative permittivity, ε_r', as a function of temperature of B0 and B20 samples.

In Fig. 4, the continuous lines correspond to the estimations and the limits of the uncertainty bands (one standard deviation) are plotted with dashed-lines. As stated before, permittivity data of DF as a function of temperature are scarce in literature.

It is worth mentioning that in the case of pure diesel fossil, B0, the uncertainty band is so narrow that its limits cannot be distinguished from the continuous line in Fig. 4.

Fig. 5 shows the projection of $\varepsilon_r'(Bx, T)$ onto the (ε_r', Bx) plane. The symbols correspond to the experimental values of permittivity and the continuous lines correspond to the first order model of Eq. (2).

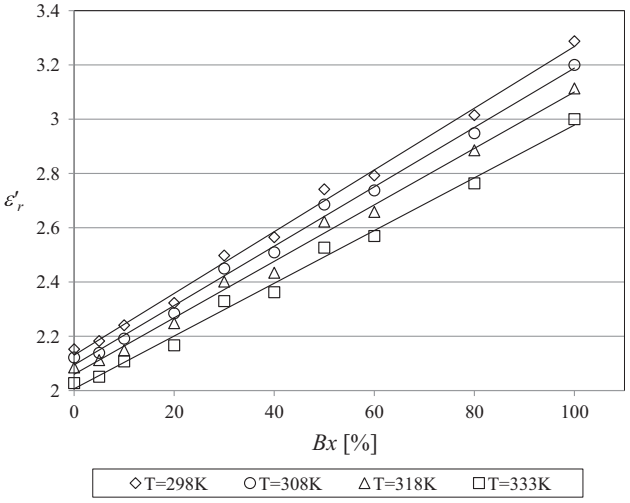

Fig. 5. Relative permittivity, ε_r', as a function biodiesel content, Bx. The lines correspond to the fitting of $\varepsilon_r'(Bx, T)$ to Eq. (2), at measurement temperatures of 298.0 K, 313.0 K, 323.0 K and 333.0 K.

Table 1
Fitting parameters of Eq. (3): $\varepsilon'_r(T_o)$ and $\delta\varepsilon'_r/\delta T$, their uncertainties $\Delta\varepsilon'_r(T_o)$ and $\Delta\delta\varepsilon'_r/\delta T$, the RMS uncertainty of the fitting, $\Delta\varepsilon'_r$, and the determination coefficient R^2. The reference temperature is T_o = 318.0 K.

Sample	$\varepsilon'_r(T_o)$	$\Delta\varepsilon'_r(T_o)$	$\delta\varepsilon'_r/\delta T \times 10^{-3}$ [K]$^{-1}$	$\Delta\delta\varepsilon'_r/\delta T \times 10^{-3}$ [K]$^{-1}$	$\Delta\varepsilon'_r$	R^2
B0	2.082	0.001	−4.0	0.1	0.003	0.997
B5	2.108	0.001	−4.0	0.1	0.004	0.993
B10	2.155	0.003	−4.0	0.3	0.007	0.979
B20	2.237	0.003	−5.0	0.2	0.007	0.990
B30	2.402	0.003	−5.0	0.1	0.007	1.000
B40	2.443	0.003	−6.0	0.3	0.008	0.990
B50	2.621	0.001	−6.0	0.1	0.004	0.998
B60	2.664	0.002	−6.0	0.3	0.006	0.996
B80	2.875	0.002	−7.0	0.3	0.006	0.997
B100	3.116	0.002	−8.0	0.2	0.006	0.997

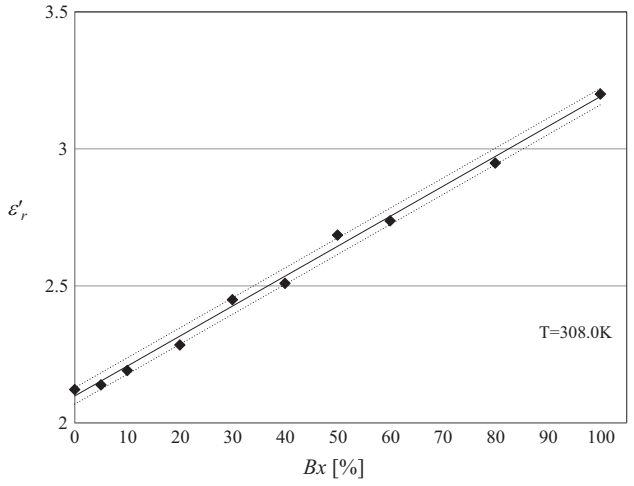

Fig. 6. Relative permittivity, ε_r', as a function of biodiesel content, *Bx*, at $T = 308.0$ K. The continuous line indicates the fitting and the dashed-lines are the limits of the uncertainty band (one standard deviation).

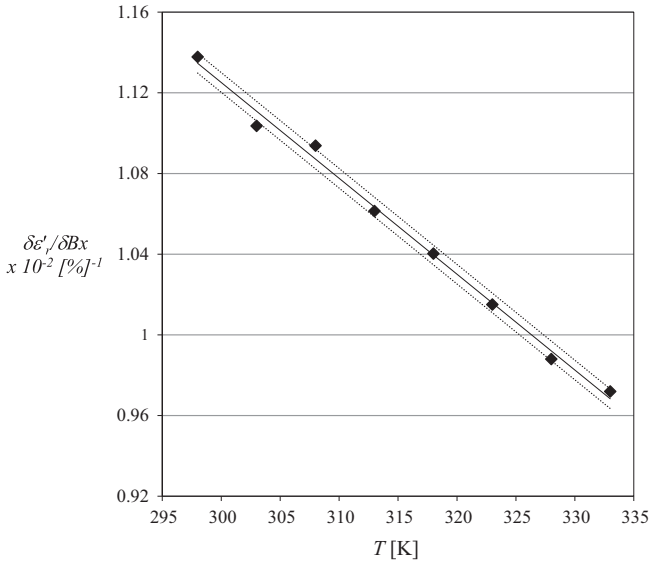

Fig. 7. $\delta\varepsilon'_r(T)/\delta Bx$ as a function of sample temperature, *T*.

Fig. 6 shows in more detail the fitting of experimental values of ε'_r (symbols) to the linear model (Eq. (2)) at $T = 308.0$ K. The continuous line indicates the fitting and the dashed-lines are the limits of the uncertainty band (one standard deviation).

From Figs. 5 and 6 it can be seen that the linear model of Eq. (2) fits very satisfactorily to the experimental data.

As explained in [18], the fittings presented in this work for biodiesel from soybean may also be applied, within the stated uncertainties, to biodiesel from other vegetable feedstocks. This was checked by recalculating the parameters of Table 4 using the values from Table II of [6]. The RMS value of the difference between the estimated permittivity values for BD from each feedstock with those presented here for BD from soybean is less than 1%. This was to be expected since the permittivity values of fresh biodiesel from feedstocks of Ref. [6] are very similar to those of fresh biodiesel from soybean. Therefore, the fittings presented in this work for fresh biodiesel from soybean may also be applied, within the stated uncertainties, to fresh biodiesel from other vegetal feedstocks.

Moreover, they also apply to used vegetable oils, if adequately treated [2,10,18].

The fitting parameters of Eq. (2), $\varepsilon'_r(B0)$ and $\delta\varepsilon'_r(T)/\delta Bx$, are given in Table 2 at each measurement temperature. Table 2 also presents the uncertainties, $\Delta\varepsilon'_r(B0)$ and $\Delta\delta\varepsilon'_r/\delta Bx$, the RMS uncertainty of the fitting, $\Delta\varepsilon'_r$, and the determination coefficient, R^2.

From Table 2 it can be noted that, in all cases, the linear model of Eq. (2) fits the experimental data very well. In fact, the uncertainty of the estimation of ε'_r is below 2% in all cases.

Fig. 7 shows the plot of $\delta\varepsilon'_r/\delta Bx$ (symbols), obtained from Table 2, as a function of the measurement temperature. The continuous line corresponds to the model of Eq. (3) and the dashed-lines indicate the limits of the uncertainty band (one standard deviation).

Table 3 shows the results of the fitting of $\delta\varepsilon'_r/\delta Bx$ to Eq. (3) including the fitting parameters, $\delta\varepsilon'_r(T_o)/\delta Bx$ and $\delta^2\varepsilon'_r(T_o)/\delta Bx\delta T$. The uncertainties, $\Delta\delta\varepsilon'_r(T_o)/\delta Bx$ and $\Delta\delta^2\varepsilon'_r(T_o)/\delta Bx\delta T$, the RMS uncertainty of the fitting, $\Delta\left(\frac{\delta\varepsilon'_r(T)}{\delta Bx}\right)$, and the determination coefficient, R^2, are also shown in the table.

It can be seen that Eq. (3) fits very satisfactorily the dependence of permittivity with composition, $\delta\varepsilon'_r(T)/\delta Bx$.

Eq. (4) can also be written as

$$\varepsilon'_r(Bx,T) = a + bT + cBx + dTBx \tag{5}$$

Coefficients *a*, *b*, *c* and *d* of Eq. (5) were determined by means of a multi-variate regression using all the experimental data. Table 4 shows the fitting values of the coefficients in Eq. (5), together with the RMS fitting uncertainty of the permittivity, $\Delta\varepsilon'_r$.

The coefficients agree very well with those calculated from Eqs. (1)–(3) using the parameters given in Tables 1–3.

Fig. 8 shows a plot of the experimental values of permittivity (black spheres) and the estimation from Eq. (5) (empty spheres) as a function of temperature, *T*, and composition, *Bx*. The agreement between the experimental values of permittivity and the estimation from Eq. (5) is very good. The very satisfactory fitting suggests the possibility of estimating the composition of DF/BD blends by means of permittivity measurements in the full composition range.

Table 2
Fitting parameters of Eq. (4): $\varepsilon_r'(B0,T)$ and $\delta\varepsilon'_r(T)/\delta Bx$, their uncertainties $\Delta\varepsilon_r'(B0,T)$ and $\Delta\delta\varepsilon'_r(T)/\delta Bx$, the RMS uncertainty of the fitting, $\Delta\varepsilon_r'$, and the determination coefficient R^2, at each measurement temperature.

Temperature [K]	$\varepsilon'_r(B0)$	$\Delta(\varepsilon'_r(B0))$	$\delta\varepsilon'_r/\delta Bx \times 10^{-2}$ [%]$^{-1}$	$\Delta(\delta\varepsilon'_r/\delta Bx) \times 10^{-2}$ [%]$^{-1}$	$\Delta\varepsilon'_r$	R^2
298	2.13	0.01	1.138	0.003	0.03	0.995
303	2.11	0.01	1.104	0.002	0.02	0.997
308	2.09	0.01	1.094	0.003	0.03	0.995
313	2.08	0.01	1.061	0.002	0.02	0.996
318	2.06	0.01	1.040	0.003	0.03	0.994
323	2.04	0.02	1.015	0.003	0.03	0.993
328	2.02	0.02	0.988	0.003	0.03	0.992
333	2.01	0.01	0.972	0.003	0.03	0.993

Table 3
Fitting parameters of Eq. (5): $\delta\varepsilon'_r(T_o)/\delta Bx$ and $\delta^2\varepsilon'_r/\delta Bx\delta T$, their uncertainties $\Delta\delta\varepsilon'_r(T_o)/\delta Bx$ and $\Delta\delta^2\varepsilon'_r(T_o)/\delta Bx\delta T$, the RMS uncertainty of the fitting, $\Delta\left(\frac{\delta\varepsilon'_r(T)}{\delta Bx}\right)$, and the determination coefficient R^2. The reference temperature is T_o = 318.0 K.

$\delta\varepsilon'_r(To)/\delta Bx \times 10^{-2}$ [%]$^{-1}$	$\Delta(\delta\varepsilon'_r(T_o)/\delta Bx) \times 10^{-2}$ [%]$^{-1}$	$\delta^2\varepsilon'_r/\delta Bx\delta T \times 10^{-5}$ [%K]$^{-1}$	$\Delta(\delta^2\varepsilon'_r/\delta Bx\delta T) \times 10^{-5}$ [%K]$^{-1}$	$\Delta(\delta\varepsilon'_r/\delta Bx) \times 10^{-2}$ [%]$^{-1}$	R^2
1.040	0.002	4.8	0.2	0.005	0.994

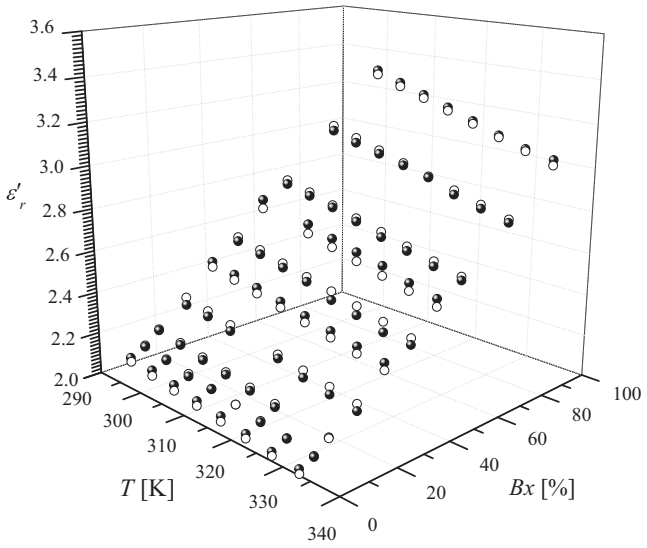

Fig. 8. Permittivity experimental data (black spheres) and estimations from Eq. (5) (empty spheres).

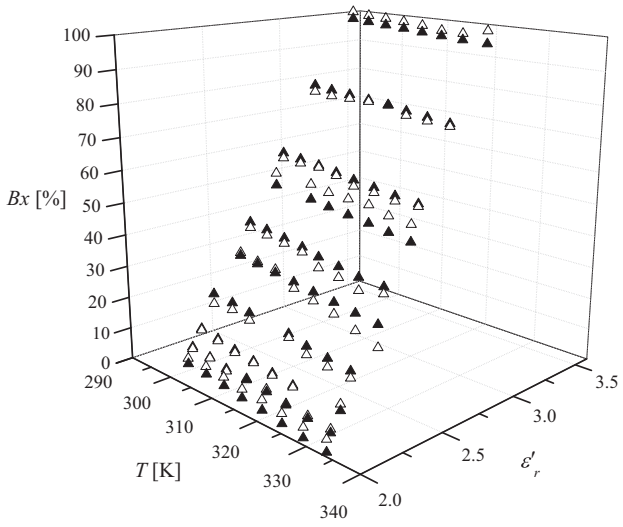

Fig. 9. Biodiesel content (black triangles) and estimations from Eq. (6) (empty triangles).

Table 4
Fitting parameters of Eq. (5) and RMS uncertainty of the permittivity estimation, $\Delta\varepsilon'_r$.

a	$b \times 10^{-3}$ [K]$^{-1}$	$c \times 10^{-2}$ [%]$^{-1}$	$d \times 10^{-5}$ [%K]$^{-1}$	$\Delta\varepsilon'_r$
3.329	−4.0	2.5	−4.5	0.03

Table 5
Fitting parameters of Eq. (6) and RMS uncertainty of the composition estimation, ΔBx.

a' [%]	$b' \times 10^{-3}$ [K]$^{-1}$	$c' \times 10^{-2}$ [%]$^{-1}$	$d' \times 10^{-5}$ [%K]$^{-1}$	ΔBx [%]
3.328	−4.0	2.5	−4.7	2.5

4.2. Estimation of the composition of diesel fossil fuel blends with biodiesel

The estimation of the composition of DF/BD blends is of interest in many technological applications. Since the model of Eq. (5) fits experimental data very satisfactorily, this suggests the following model to estimate the biodiesel content from permittivity and temperature measurements,

$$B_x(\varepsilon'_r, T) = \frac{\varepsilon'_r - a' - b'T}{c' + d'T} \tag{6}$$

The parameters of Eq. (6) were determined by means of a multiple non-linear regression performed on this equation using all the experimental data. Table 5 shows the fitting values of the coefficients and the RMS uncertainty of the fitting of the composition estimation, ΔBx.

It must be remarked that the coefficients from Tables 4 and 5 agree very well. Fig. 9 shows the composition of the samples (black triangles) and the estimation from Eq. (6) (empty triangles) as a function of temperature and permittivity. It may be seen that Eq. (6) estimates Bx very satisfactorily as a function of ε'_r and T. The RMS uncertainty was below 2.5% in the full range of temperatures and compositions.

This accurate results may be obtained in real-time from a sensor placed after the fuel filtering system of a Diesel vehicle and used as an input for an electronic management unit (EMU) for the optimization of the combustion parameters in the engine. This is very important in order to optimize fuel consumption and to comply with emissions limits.

5. Conclusions

The relative permittivity of diesel fuel and blends with biodiesel from soybean oil was determined with an airtight cell, for the full composition range at temperatures between 298.0 K and 333.0 K (controlled within ±0.1 K), at frequencies from 1 kHz to 100 kHz. This frequency range is suitable for the use of low-cost, portable equipment and also for the development of automotive sensors. The measurement uncertainty of the permittivity data was below 1%. As it was to be expected from previous works, the permittivity

did not depend on frequency; therefore, all the results presented in this work correspond to a frequency of 100 kHz. Measurements at this frequency minimize the influence of electrodes polarization, that could alter the results in the case of conductive (deficiently purified) samples.

At each composition, the relative permittivity decreases linearly with temperature and, at constant temperature, increases linearly with biodiesel content.

From these results, a simple model was proposed to estimate the permittivity of the samples as a function of biodiesel content and temperature in the full composition range. Experimental data agreed very well with the model; the RMS uncertainty of the estimation was below 1.2%. This extends previously reported results for biodiesel-rich blends.

The very satisfactory fitting suggested that it was possible to estimate the composition of blends from permittivity and temperature measurements. The model parameters for the estimation were independently determined by a multiple non-linear regression analysis using all the experimental data. The RMS uncertainty of the composition estimation was below 2.5% in the full studied range.

In conclusion, dielectric measurements at 100 kHz may be applied to estimate accurately the composition of diesel/biodiesel blends in the temperature range from 298 K to 333 K.

Acknowledgments

This work was supported by Project UBACyT 20020120100062BA, CONICET PIP 0241, UBACyT 20020120100025BA, UBACyT 20020130100346BA and UBACyT 20020120100051BA, of the Universidad de Buenos Aires (UBA). The authors thank Mr. Miguel Pellejero, Eng., (YPF Fuel Developing Laboratory) and Mr. Sergio Bergerman, Eng., (Shell CAPSA – Refinería Buenos Aires) for the samples of diesel fuel.

References

[1] Knothe G, Krahl J, Van Gerpen J. The biodiesel handbook. 2nd ed. Urbana: AOCS Press; 2010.
[2] Romano SD, Sorichetti PA. Dielectric relaxation spectroscopy in biodiesel production and characterization. 1st ed. London: Springer Verlag; 2011.
[3] Romano SD, González Suárez E, Laborde MA. Combustibles alternativos. 2nd ed. Buenos Aires: Ediciones Cooperativas; 2006.
[4] Munack A, Speckmann H, Krahl J, Marto A, Bantzhaff R. A sensor for discrimination of fossil diesel fuel, biodiesel, and their blends. In: Knothe G, Krahl J, Van Gerpen J, editors. The biodiesel handbook. Urbana: AOCS Press; 2010. p. 131–6.
[5] Tat M, Van Gerpen J. Measurement of biodiesel speed of sound and its impact on injection timing. National Renewable Energy Laboratory; 2003. NREL/SR-510-31462.
[6] Corach J, Sorichetti PA, Romano SD. Electrical and ultrasonic properties of vegetable oils and biodiesel. Fuel 2015;139:466–71.
[7] Lizhi H, Toyoda K, Ihara I. Dielectric properties of edible oils and fatty acids as a function of frequency, temperature, moisture and composition. J Food Eng 2008;88:151–8.
[8] Corach J, Sorichetti PA, Romano SD. Electrical properties of vegetable oils between 20 Hz and 2 MHz. Int J Hydrogen Energy 2014;39:8754–8.
[9] Romano SD, Sorichetti PA, Buesa Pueyo I. Methanol content in biodiesel estimated by flash point and electrical properties. In: Erbaum JB, editor. Bioethanol: production, benefits and economics. New York: NOVA Science Publishers Inc.; 2009. p. 135–46.
[10] Sorichetti PA, Romano SD. Physico-chemical and electrical properties for the production and characterization of biodiesel. Phys Chem Liq 2005;43 (1):37–48.
[11] Gonzalez Prieto LE, Sorichetti PA, Romano SD. Electric properties of biodiesel in the range from 20 Hz to 20 MHz. Comparison with diesel fossil fuel. Int J Hydrogen Energy 2008;33:3531–7.
[12] Corach J, Sorichetti PA, Romano SD. Electrical properties of mixtures of fatty acid methyl esters from different vegetable oils. Int J Hydrogen Energy 2012;37(19):14735–9.
[13] M'Peko JC, Reis DLS, De Souza JE, Caires ARL. Evaluation of the dielectric properties of biodiesel fuels produced from different vegetable oil feedstocks through electrochemical impedance spectroscopy. Int J Hydrogen Energy 2013;38(22):9355–9. 105.
[14] Murari MR, Wilson W, Majed A. Performance and emissions of a diesel engine fueled by biodiesel–diesel, biodiesel–diesel-additive and kerosene–biodiesel blends. Energy Convers Manage 2014;84:164–73.
[15] ASTM D7371-14. Standard Test Method for Determination of Biodiesel (Fatty Acid Methyl Esters) Content in Diesel Fuel Oil Using Mid Infrared Spectroscopy (FTIR-ATR-PLS Method); 2014.
[16] Tat ME, Van Gerpen JH. Biodiesel blend detection using a fuel composition sensor. In: ASAE Annual International Meeting; 2001. <http://web.cals.uidaho.edu/biodiesel/files/2013/08/ASABE-01-6052.pdf>.
[17] De Souza JE, Scherer MD, Cáceres JAS, Caires ARL, M'Peko JC. A close dielectric spectroscopic analysis of diesel/biodiesel blends and potential dielectric approaches for biodiesel content assessment. Fuel 2013;105:705–10.
[18] Corach J, Sorichetti PA, Romano SD. Permittivity of biodiesel-rich blends with fossil diesel fuel: application to biodiesel content estimation. Fuel 2016;177:268–73.
[19] EN 14214 (European standard for biodiesel): automotive fuels – fatty acid methyl esters (FAME) for diesel engines – requirements and test methods; 2008.
[20] ASTM D975-15c. Standard specification for diesel fuel oils; 2015.
[21] Sorichetti PA, Matteo CL. Low-frequency dielectric measurement of complex fluids using high-frequency coaxial sample cells. Measurement 2007;40 (4):437–49.
[22] Kremer F, Schonhals A. Broadband dielectric spectroscopy. 1st ed. Berlin, Heidelberg: Springer-Verlag; 2003.